

Effect of strontium oxide on radiation attenuation properties of boro-tellurate glass systems at high radiation energies

S. Mthalande¹, B. Bhengu¹, N. Msabala¹, M.N Zuma¹, C.B Mtshali², H.A.A Abdelbagi¹, T.T Hlatshwayo³, S. S. Ntshangase¹

¹Physics Department, University of Zululand, KwaDlangezwa, 3886, South Africa

²Materials Research Department, iThemba LABS, P.O. Box 722, Somerset West, 7129, South Africa

³Physics Department, University of Pretoria, Pretoria, 0002, South Africa

Email: msifiso999@gmail.com

Abstract. In the present study, the radiation shielding properties of five glass compositions 40SrO–30B₂O₃–10TeO₂–20Bi₂O₃, 35SrO–30B₂O₃–10TeO₂–25Bi₂O₃, 30SrO–30B₂O₃–10TeO₂–30Bi₂O₃, 25SrO–30B₂O₃–10TeO₂–35Bi₂O₃, and 20SrO–30B₂O₃–10TeO₂–40Bi₂O₃, were investigated using Phy-X/PSD software, and validated through GEANT4 simulations. The mass attenuation coefficients (MAC), linear attenuation coefficients (LAC), and effective atomic numbers of the glasses were determined across the energy range of 1–15 MeV. Results showed that increasing the Bi₂O₃ while decreasing SrO content enhances the radiation shielding capability of the glasses. Additionally, the half-value layer (HVL), and tenth-value layer (TVL), were evaluated, revealing that glasses with higher Bi₂O₃ concentrations attenuate a greater amount of photons with smaller thicknesses. 20SrO–30B₂O₃–10TeO₂–40Bi₂O₃ glass demonstrated superior radiation shielding performance and can be used in both nuclear and medical applications.

1 Introduction

The increasing usage of ionizing radiation across the industrial, medical, food, and research sectors has become significantly vital to modern economic, social, and technological advancements. However, despite its significance, ionizing radiation raises serious safety concerns due to its risks to human health [1, 2]. Therefore, it is crucial to develop effective preventative measures to minimize radiation exposure and safeguard individuals from its harmful effects. In the past few decades, various shielding materials have been developed and implemented to reduce ionizing radiation exposure, with lead (Pb) and concrete being among the most employed materials. These materials have been favoured due to their high density and high linear attenuation coefficients (LAC), which enable them to effectively attenuate ionizing radiation [3,4]. Nevertheless, lead is a highly toxic metal known to negatively impact human health. On the other hand, concrete can offer effective radiation shielding under certain conditions, but it also has notable limitations [3,5,6]. For example, if the water content in concrete exceeds optimal levels, its structural strength decreases, and its overall density is reduced. Additionally, in high-temperature environments, the absorbed radiation energy can cause the water to evaporate [5,7,8]. This not only compromises the structural integrity of the concrete, but also leads to cracking, which can allow ionizing radiation to penetrate, thereby posing significant health risks to humans. Considering these limitations of concrete, along with the toxic nature of lead (Pb), researchers have increasingly turned their focuses to developing an alternative material to replace both concrete and lead in radiation shielding applications.

In recent years, researchers have increasingly focused on glass materials due to their excellent physical properties, optical properties, resistance to corrosion, light weight, non-toxicity and radiation shielding properties [4,6-8]. One of the main reasons for glass materials to be preferred for specialized applications such as in environments like nuclear laboratories is their inherent transparency. This property allows glass to serve as effective radiation shielding while allowing observers to monitor activities inside areas containing ionizing radiation sources.

There are several types of glass formers, such as tellurium dioxide (TeO_2), boron oxide (B_2O_3), germanium dioxide (GeO_2), and silica (SiO_2) which are the glass network backbones. These glass formers can be combined with various modifiers, such as heavy metal oxides (HMOs) and light metal oxides (LMO) [6,9]. Added HMOs or (LMO) to glass formers can particularly increase the density of the glass and its atomic number, thereby enhancing its ability to attenuate radiation, which is an essential characteristic for applications requiring effective shielding [5,9]. Thabet *et al.* [7] studied the gamma-ray shielding capability of $x\text{Bi}_2\text{O}_3 + (75-x)\text{B}_2\text{O}_3 + 15\text{TeO}_2 + 5\text{MgO} + 5\text{PbO}$; $x = 0, 10, 20, 25, 30, 40, 50, 60$], where the shielding properties of these glasses were improved by increasing bismuth oxide (Bi_2O_3) content. Moreover, Kaky *et al.* [8] investigated the influence of Bi_2O_3 on gamma-ray attenuation properties of the following glass system: $(50-x)\text{B}_2\text{O}_3 + 5\text{SiO}_2 + 40\text{MgO} + x\text{Bi}_2\text{O}_3$, where $x = 5, 10, 15$, and 20. As a result of these results, it is evident that adding more Bi_2O_3 further improves radiation attenuation in the glass system.

Recently, the mechanical, structural, and radiation shielding properties of boro-tellurite glasses modified by varying concentrations of strontium and bismuth oxides have been investigated for photon energies below 0.81 MeV [6]. Therefore, it is critical to observe the behaviour of this glass system in energy regions above 0.81 MeV, which is the main purpose of this work. This study investigates the gamma-ray attenuation properties of boro-tellurite glasses modified with varying concentrations of strontium and bismuth oxides, using Geant4 simulations. The results were also analysed using Phy-x\PSD software to evaluate key shielding parameters, including the linear attenuation coefficient (LAC), mass attenuation coefficient (MAC), half-value layer (HVL), tenth-value layer (TVL), mean free path (MFP), and effective atomic number (Z_{eff}) of the glass system used in this study.

2 Experimental Methods

The radiation shielding properties of glass systems with compositions $40\text{SrO} + 30\text{B}_2\text{O}_3 + 10\text{TeO}_2 + 20\text{Bi}_2\text{O}_3$, $35\text{SrO} + 30\text{B}_2\text{O}_3 + 10\text{TeO}_2 + 25\text{Bi}_2\text{O}_3$, $30\text{SrO} + 30\text{B}_2\text{O}_3 + 10\text{TeO}_2 + 30\text{Bi}_2\text{O}_3$, $25\text{SrO} + 30\text{B}_2\text{O}_3 + 10\text{TeO}_2 + 35\text{Bi}_2\text{O}_3$, and $20\text{SrO} + 30\text{B}_2\text{O}_3 + 10\text{TeO}_2 + 40\text{Bi}_2\text{O}_3$ were evaluated using Phy-X/PSD software. In addition, Phy-X/PSD results were compared with Geant4 Monte Carlo Simulations (MCS) results. The Geant4 (MCS) framework offers several advantages, most notably its flexibility in designing and simulating complex experimental setups, such as the gamma radiation source, glass samples, detectors, and collimators within a computational environment. The glass codes, glass compositions and density of the investigated glasses are shown below in Table 1, taken from [6].

Table 1: The investigated glass samples and their densities.

Glass code	Glass compositions	Density (g/cm^3)
TBSB1	$40\text{SrO} + 30\text{B}_2\text{O}_3 + 10\text{TeO}_2 + 20\text{Bi}_2\text{O}_3$	4.32
TBSB2	$35\text{SrO} + 30\text{B}_2\text{O}_3 + 10\text{TeO}_2 + 25\text{Bi}_2\text{O}_3$	4.65
TBSB3	$30\text{SrO} + 30\text{B}_2\text{O}_3 + 10\text{TeO}_2 + 30\text{Bi}_2\text{O}_3$	5.07
TBSB4	$25\text{SrO} + 30\text{B}_2\text{O}_3 + 10\text{TeO}_2 + 35\text{Bi}_2\text{O}_3$	5.40
TBSB5	$20\text{SrO} + 30\text{B}_2\text{O}_3 + 10\text{TeO}_2 + 40\text{Bi}_2\text{O}_3$	5.69

Radiation shielding parameters such as the mass attenuation coefficient (MAC), linear attenuation coefficient (LAC), half-value layer (HVL), tenth-value layer (TVL), and effective atomic number (Z_{eff}) are crucial for ensuring shielding materials efficiency. Therefore, the accurate determination of these factors is essential for the development of efficient shielding materials aimed at reducing gamma radiation exposure.

A fundamental parameter in assessing shielding effectiveness is the mass-attenuation coefficient (MAC). The MAC quantifies the material's capacity to attenuate or reduce the intensity of incident gamma radiation as it traverses the substance. It is energy-dependent and closely related to material density, however a material with a higher atomic number typically exhibits greater MAC values. A higher MAC indicates that a material is more effectively shielded from radiation per unit mass, showing superior attenuation performance. The MAC is also closely related to the LAC and serves as its density-independent counterpart. The MAC can be calculated using the following formula [4,5]:

$$\text{MAC} = \frac{\mu}{\rho} \quad (1)$$

where μ is the LAC and ρ is the density of the material. The LAC represents the fraction of gamma radiation attenuated per unit thickness of a material. A higher LAC value indicates that the material is more effective at reducing the intensity of incoming photons. In other words, materials with high LAC values are better at shielding radiation. The LAC can be calculated using the following formula [4,5]:

$$I = I_0 e^{-\mu t} \quad (2)$$

where t represents the thickness of the material, I_0 denotes the initial radiation intensity before entering the material, and I is the intensity of the radiation after transmission through the material.

Another important radiation shielding parameters are the half-value layer (HVL) and tenth-value layer (TVL), which are defined as the thickness of a material required to reduce the intensity of incoming radiation by 50% and 90%, respectively. Lowest HVL and TVL values indicate better shielding efficiency. The HVL and TVL can be calculated using the following formula [4,5]:

$$\text{HVL} = \frac{\ln(2)}{\mu} \quad (3)$$

and

$$\text{TVL} = \frac{\ln(10)}{\mu} \quad (4)$$

The last parameter considered in the study is the effective atomic number Z_{eff} which plays an important role in evaluating the radiation shielding properties of a material. The Z_{eff} represents the average atomic number taking into account the contribution of all constituent elements to its composition. The Z_{eff} depends on the type of radiation and the interactions between the particles and the material. A higher Z_{eff} value indicates a greater ability to attenuate radiation, making the material more effective as a shielding material. The effective atomic number can be calculated using the following formula [4,5]:

$$Z_{\text{eff}} = \frac{\sum f_i A_i \left(\frac{\mu}{\rho}\right)_i}{\sum f_i \left(\frac{A_i}{Z_i}\right) \left(\frac{\mu}{\rho}\right)_i}, \quad (5)$$

where f_i , A_i , and Z_i represent the mole fraction, atomic weight, and atomic number of each element, respectively, in the absorber material.

3 Results and discussion

The selected $\text{SrO} + \text{B}_2\text{O}_3 + \text{TeO}_2 + \text{Bi}_2\text{O}_3$ glass systems were evaluated for their radiation attenuation performance by calculating several shielding parameters in the energy range of 1 to 15 MeV. In this study, the linear attenuation coefficient (LAC) was the first radiation-shielding parameter assessed as a function of photon energy. Figure 1 illustrates the LAC profile for the $\text{SrO}-\text{B}_2\text{O}_3-\text{TeO}_2-\text{Bi}_2\text{O}_3$ glass system across a photon energy from 1 to 15 MeV. As shown in Figure 1, the LAC of the glass system decreases exponentially as the photon energy increases from 1 to 6 MeV and slowly increases as the photon energy goes from 6 MeV to 15 MeV. This exponential decrease of the LAC is due predominately to Compton effect, which takes place as photon energy increases, where around 6 MeV the pair production starts to be dominant up until 15 MeV. This behaviour of LAC values as a function of photon energy has also been observed in the literature [4]. Furthermore, it can be noticed that TBSB1 exhibits the lowest LAC while TBSB5 exhibits the highest LAC value. In particular, within the energy range of 1 to 15 MeV, LAC value falls within the range of 0.2724 to 0.173 cm^{-1} , 0.297 to 0.194 cm^{-1} , 0.329 to 0.209 cm^{-1} , 0.354 to 0.228 cm^{-1} , 0.377 to 0.237 cm^{-1} , for TBSB1, TBSB2, TBSB3, TBSB4 and TBSB5, respectively. The trend of decreasing LAC from TBSB5 to TBSB1 highlights that increasing the Bi_2O_3 content

while reducing the SrO content leads to a lower LAC. Same behaviour was observed in a previous study where increasing Bi₂O content resulted in a higher LAC value [8].

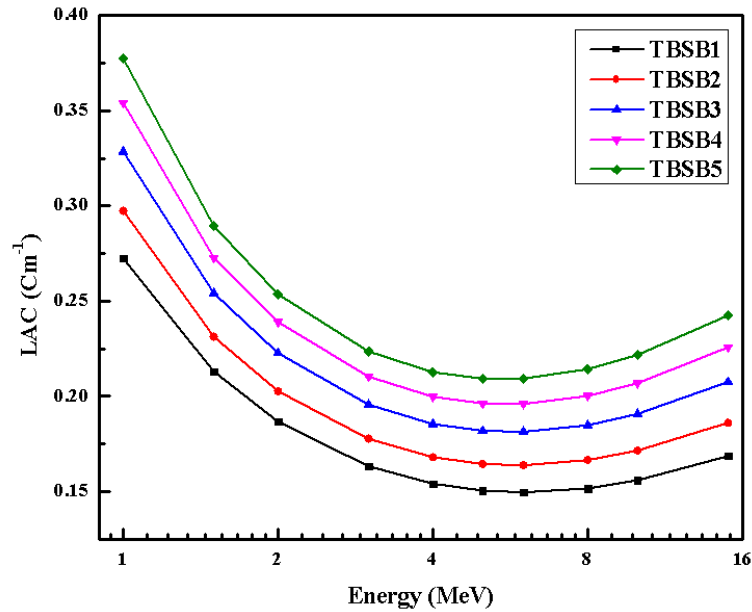


Figure 1: Linear attenuation coefficients (LAC) for the TBSB1TBSB5 glass samples.

The MAC values calculated using Phy-X/PSD align closely with those from Geant4 MC simulations, as shown in Table 2. These theoretical results demonstrate consistent agreement across all glass samples (TBSB1–TBSB5). Comprehensive validation studies confirm the reliability of Phy-X/PSD and Geant4 simulations, supported by experimental data in [4,6]. Therefore, the MAC values and related parameters derived from Phy-X/PSD are deemed accurate when compared with the experimental results, reinforcing their utility for analysis. Notably, the MAC value decreases as the photon energy increases, indicating more photon interactions at lower energies (e.g., 1 MeV) and fewer interactions at higher energies, allowing more gamma-ray photons to pass through the material. It can also be observed that glass samples TBSB1 have low MAC values and TBSB5 have higher MAC values. This may be due to decreasing the content of SrO while increasing Bi₂O₃.

Table 2: Comparison between MAC values obtained from Geant4 simulations and Phy-X/PSD calculations for TBSB1-TBSB5 glass samples.

Energy (MeV)	MAC (cm ² /g), TBSB1		MAC (cm ² /g), TBSB2		MAC (cm ² /g), TBSB3		MAC (cm ² /g), TBSB4		MAC (cm ² /g), TBSB5	
(MeV)	Geant4	Phy-X/PSD	Geant4	Phy-X/PSD	Geant4	Phy-X/PSD	Geant4	Phy-X/PSD	Geant4	Phy-X/PSD
1	0.061	0.063	0.061	0.064	0.061	0.064	0.066	0.063	0.066	0.063
1.5	0.048	0.049	0.048	0.050	0.049	0.050	0.051	0.049	0.051	0.050
2	0.042	0.043	0.042	0.043	0.043	0.044	0.044	0.043	0.044	0.043
3	0.037	0.038	0.036	0.038	0.037	0.039	0.039	0.038	0.044	0.038
4	0.034	0.036	0.034	0.036	0.034	0.036	0.037	0.035	0.039	0.036
5	0.033	0.036	0.033	0.035	0.033	0.036	0.036	0.034	0.038	0.035
6	0.033	0.034	0.033	0.035	0.033	0.036	0.036	0.034	0.037	0.034
8	0.033	0.035	0.033	0.035	0.033	0.035	0.036	0.034	0.037	0.034
10	0.034	0.036	0.034	0.037	0.034	0.038	0.038	0.034	0.039	0.035
15	0.036	0.039	0.037	0.040	0.037	0.040	0.042	0.037	0.042	0.038

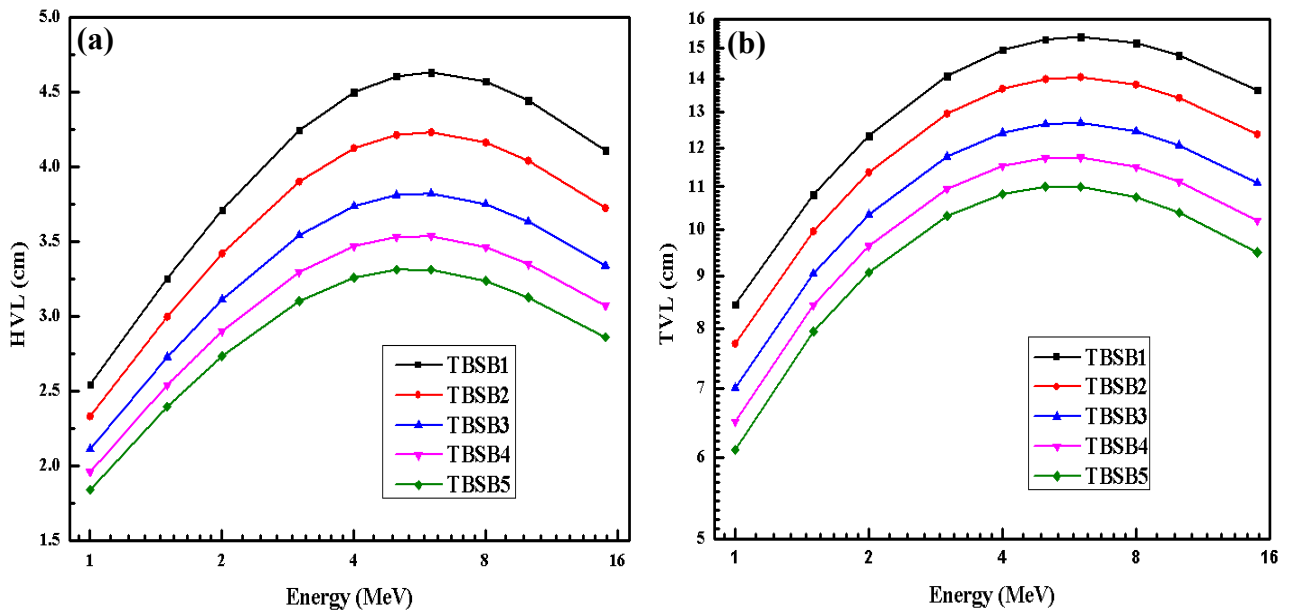


Figure 2: (a) Half value layer (HVL) and (b) tenth value layer (HVL) for the TBSB1 to TBSB5 glass samples.

Figure 2 (a) and (b) show HVL and TVL, respectively, as a function of photon energy, for the five glass samples studied. From Figure 2, it can be observed that the glass TBSB5 has the lowest TVL and HVL, whereas TBSB1 has the highest TVL and HVL. For instance, within the energy range of 1 to 15 MeV, the TVL is within the interval 8.453 to 13.66 cm, 7.743 to 12.376 cm, 7.006 to 11.093 cm, 6.504 to 10.202 cm, 6.1 to 9.495 cm, for TBSB1, TBSB2, TBSB3, TBSB4, TBSB5, respectively. On the other hand, within the energy range of 1 to 15 MeV, the HVL is 2.544 to 4.112 cm, 3.331 to 3.737 cm, 2.113 to 3.343 cm, 1.962 to 3.071 cm, 1.843 to 2.857 cm, for glass TBSB1, TBSB2, TBSB3, TBSB4, TBSB5, respectively. These results show that the TVL and HVL of these five glass systems decrease as the content of SrO decreases while Bi_2O_3 increases. It can be observed that the TVL and HVL when the photon energy is around 5 MeV the trend starts to change and slowly decreases. This was also observed in the literature in [8].

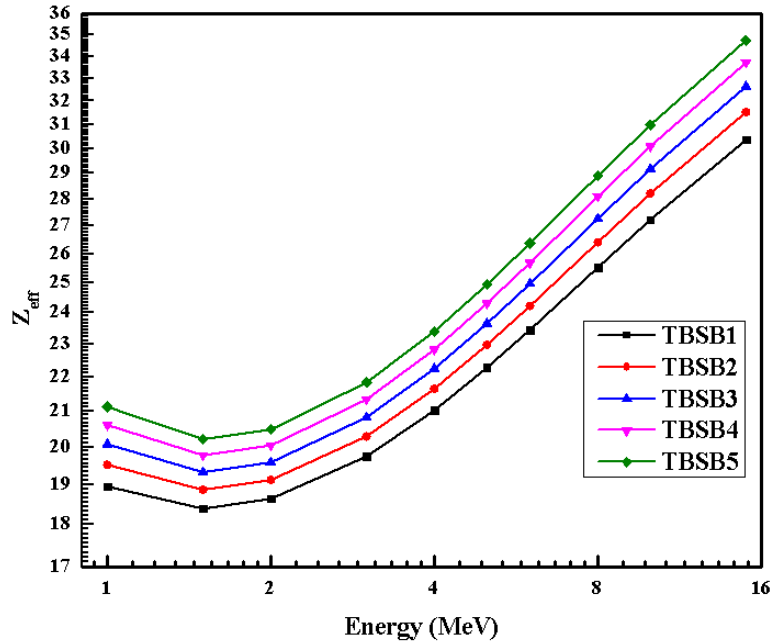


Figure 3: Effective atomic number for the TBSB1-TBSB5 glass samples.

Figure 3 shows the variation of the effective atomic number (Z_{eff}) as a function of photon energy for glass samples from TBSB1 to TBSB5. From Figure 4 it can be seen that from 1 to 1.5 MeV the Z_{eff} decrease for all glass samples. This is due to the predominant Compton effect in this energy region. Similar behaviour was observed in the literature in [4,5]. As depicted in Figure 4, from 1.5 MeV the Z_{eff} increases with an increase in photon energy. Throughout the energy range of 1.5 to 15 MeV, a steady increase in Z_{eff} is observed across all glass systems. This gradual increase of Z_{eff} show that there are more electrons available for photon interaction, which shows that there is possibility for photons to interact with the material in the energy range from 1.5 to 15 MeV. The same behaviour has been observed in the literature in [9,10].

4 Conclusion

The gamma-ray shielding properties of glass systems 40SrO–30B₂O₃–10TeO₂–20Bi₂O₃, 35SrO–30B₂O₃–10TeO₂–25Bi₂O₃, 30SrO–30B₂O₃–10TeO₂–30Bi₂O₃, 25SrO–30B₂O₃–10TeO₂–35Bi₂O₃, and 20SrO–30B₂O₃–10TeO₂–40Bi₂O₃ were investigated using Phy-X/PSD software and validated with Geant4 MC simulations. The mass attenuation coefficient (MAC) results obtained from Phy-X/PSD showed good agreement with those obtained from Geant4 MC simulations. The linear attenuation coefficient (LAC), half-value layer (HVL), tenth-value layer (TVL), and effective atomic number (Z_{eff}) were calculated using Phy-X/PSD. Among the compositions studied, glass with 20SrO–30B₂O₃–10TeO₂–40Bi₂O₃ exhibited the highest MAC, LAC, and Z_{eff} values, along with the lowest HVL and TVL values compared to the other glass samples, indicating superior radiation shielding performance over the other glass samples. The results indicate that decreasing the SrO content and increasing the Bi₂O₃ content enhance the gamma-ray shielding performance of the 20SrO–B₂O₃–TeO₂–Bi₂O₃ glass system within the energy range between 1 and 15 MeV. Therefore, boro-tellurite glass systems doped with high Bi₂O₃ and low SrO concentrations show strong potential for use in gamma-ray shielding applications within the 1–15 MeV energy range.

Acknowledgements

The authors thank the National research foundation, iThemba Labs and the Universities of Zululand for supporting this work.

References

- [1] D. A. Alorain, A. H. Almuqrin, M. Sayyed, and M. Elsafi, Impact of wo₃ and bao nanoparticles on the radiation shielding characteristics of polydimethylsiloxane composites, *e-Polymers* 23, 20230037 (2023).
- [2] Sharma, G. Reddy, L. Varshney, H. Bharathkumar, K. Vaze, A. Ghosh, H. Kushwaha, and T. Krishnamoorthy, Experimental investigations on mechanical and radiation shielding properties of hybrid lead–steel Fiber reinforced concrete, *Nuclear Engineering and Design* 239, 1180 (2009).
- [3] H. Alrebdi, A. Almuqrin, M. Hanfi, M. Sayyed, and K. Mahmoud, Influence of the SrO insertion to a binary PbO–B₂O₃ glass system: Mechanical properties and radiation shielding study, *Transactions of the Indian Ceramic Society* 81, 76 (2022).
- [4] M. Al-Buriahi, E. M. Bakhsh, B. Tonguc, and S. B. Khan, Mechanical and radiation shielding properties of tellurite glasses doped with ZnO and NiO, *Ceramics International* 46, 19078 (2020).
- [5] S. A. Issa, A. Ene, H. M. Zakaly, et al., Evaluating the effectiveness of tellurium-molybdenum oxide glass systems for radiation shielding protection, *Multidisciplinary Materials Chronicles* 1, 19 (2024).
- [6] N. Alonizan, M. Mhareb, K. Mahmoud, M. Sayyed, N. Dwaikat, Q. Drmosh, M. Y. Alqahtani, and N. A. Saleh, Mechanical, structural, and radiation shielding characteristics for transparent boro-tellurite glasses modified with strontium and bismuth oxide ratios, *Optical Materials* 146, 114524 (2023).
- [7] H. A. Thabit, M. Sayyed, F. O. Okoh, S. Yasmin, M. Kamislioglu, et al., Impact of bi₂o₃ on the glass system B₂O₃–TeO₂–MgO–PbO on the purpose of radiation shielding efficacy, *Progress in Nuclear Energy* 173, 105240 (2024).
- [8] K. M. Kak, M. Sayyed, M. K. Hamad, S. Biradar, M. Mhareb, U. Altimari, and M. M. Taki, Bismuth oxide effects on optical, structural, mechanical, and radiation shielding features of borosilicate glasses, *Optical Materials* 155, 115853 (2024).
- [9] M. Ouis and H. ElBatal, Comparative studies of ir spectra, optical and thermal properties of binary CdO–B₂O₃, SrO–B₂O₃, and BaO–B₂O₃, *Silicon* 9, 703 (2017).
- [10] R. El-Mallawany, M. Sayyed, M. Dong, and Y. Rammah, Simulation of radiation shielding properties of glasses contain Pbo, *Radiation Physics and chemistry* 151, 239 (2018).